Integrated computational strategies for UV/vis spectra of large molecules in solution

Vincenzo Barone*[a] and Antonino Polimeno[b]

Received 10th April 2007
First published as an Advance Article on the web 9th May 2007
DOI: 10.1039/b515155b

In recent years, the margin of interaction between computational chemistry and most branches of experimental chemistry has increased at a fast pace. The experimental characterization of new systems relies on computational methods for the rationalization of structural, energetic, electronic and dynamical features. In particular, novel computational approaches allow accurate estimates of molecular parameters from spectroscopic optical observables, giving rise to synergic interactions between experimentalists and theoretically-oriented chemists. Our main objective in this *tutorial review* is to delineate the degree of advancement of possible integrated computational approaches to the interpretation of optical spectroscopies, with an accent on large molecules in solvated environments, based on the combination of advanced quantum mechanical treatments and stochastic modelling of relaxation processes.

Introduction

Theoretical interpretation *via* computational modelling of optical spectroscopic observables in solution is of fundamental importance to gather information on the stability and reactivity of a molecular system. It is in fact nowadays possible to model with a relatively high accuracy physico-chemical properties of complex molecules in solution, and to link spectroscopic evidences directly to structural and dynamic properties of optically active solvated probes. For medium to large-size molecules, methods rooted in the density functional theory (DFT)[1] are paving the route toward an accurate and effective computation of structural, electric, and magnetic properties.[2] After great success for ground state properties, implementation of the powerful time-dependent extension of DFT (TD-DFT) is extending the field of application for effective linear scaling methods to excited electronic states.[1] An effective computational strategy for the study of large biochemical systems in solution can then be obtained using these DFT approaches in mixed quantum-mechanical/molecular-mechanical (QM/MM) methods and including last generation mean field models (*e.g.* the so called polarizable continuum model, PCM[3]) for the description of environmental effects.

[a]*Dipartimento di Chimica, Università di Napoli "Federico II", Complesso Univ. Monte S. Angelo, via Cintia, I-80126 Napoli, Italy. E-mail: baronev@unina.it; Fax: +39081674090; Tel: +39081674206*
[b]*Dipartimento di Scienze Chimiche, Università di Padova, via Marzolo 1, Padova, Italy. E-mail: antonino.polimeno@unipd.it; Tel: +390498275146*

Current theoretical approaches to spectroscopy in solution

The integrated DFT/MM/PCM approach has proved useful in the determination of molecular properties from ground state characteristics (geometry, charge distributions *etc.*) to spectroscopic parameters (*e.g.* magnetic tensors) to electronic excited states in solution.[4] In some instances, however, the

Vincenzo Barone

Department of Chemistry - Università degli Studi di Napoli Federico II. Born in Ancona in 1952. Full Professor in Physical Chemistry since November 1994. President of the Physical Chemistry Division of the Italian Chemical Society (2007–2009). Author of about 400 publications with about 10 000 citations. His activity is devoted to the development of new density functionals, continuum solvent models and dynamic methods and to their application to the structure and properties of complex systems (materials, nanostructures, biomolecules).

Antonino Polimeno

Department of Chemistry - Università degli Studi di Padova. Born in Turin in 1963. Associate Professor at the Università degli Studi di Padova since 2001. His activity is devoted to liquids theory, modelling of charge transfer phenomena in condensed phases and interpretation of magnetic resonance and optical spectroscopic data in soft materials and biological substrates (proteins). He is also working in the field of micro and nano fluidodynamics via non-linear fluctuating hydrodynamic and dissipative particle dynamics approaches.

representation of the solvent by a polarizable continuum may display limitations, *e.g.* in situations when highly specific interactions, like hydrogen bonds, come into play. At present, no simple recipe can be provided for these problem cases, and the set-up and validation of suitable protocols represent an area of active research. Cluster approaches can provide a straightforward route to describe the influence of solvent molecules on localized phenomena, including the spectroscopic transitions of organic molecules, while the PCM can be brought into play to account for the "bulk" solvent. The resulting cluster–PCM description[5] represents a very versatile tool that can be adapted to different structural and spectroscopic situations. The cluster–PCM approach is also attractive for the computation of averaging effects brought about by dynamics. Physically, when a spectroscopic transition is fast with respect to the time-scale of a dynamical phenomenon, the measured energetic parameters of the transition represent weighted averages over different configurations, which can be generated by a representative dynamical simulation. Averaging of the computed values provides an estimate of the measured transition position and of its line-width.[6] As far as the nature of the simulation is involved, the advantages of classical molecular dynamics are obvious, but a number of difficulties are often met, related to the quality of available force fields. As an alternative, classical simulations employing *ab initio* computed energies, *i.e.* Born–Oppenheimer dynamics and, especially, extended Lagrangian approaches like Car–Parrinello[7] and ADMP,[8] are starting to provide dynamical trajectories which are long enough to allow for reasonable averaging of some spectroscopic parameters. Note that different boundary conditions (periodic, PBC; and non-periodic, NPBC) are more suitable for a delocalized (plane-waves) or localized (*e.g.* Gaussian functions) basis set. While periodic implementations have a long history, the corresponding non-periodic algorithms are much more recent, albeit very promising.[9] A more subtle correction related to dynamical effects is due to vibrational averaging of spectroscopic parameters. Recent algorithmic improvements[10] allow for an effective computation of such vibrational averages, which have been shown to significantly influence spectroscopic parameters in a number of important cases.[11]

A truly effective and self-consistent treatment of long range dynamic solvation effects is relatively less advanced. Relevant efforts have been made in the direction of the evaluation of dynamic effects on optic observables *via* the application of stochastic models, which essentially model relaxation processes, like molecular tumbling, local solvent relaxation, internal conformational motions and so on in terms of suitable classic time evolution operators which depend upon phenomenological dissipative parameters. Brownian theory of rotational motion of molecules in liquids is a time-honoured approach which has been recently extended with the purpose of describing the effects of the local solvent structure in the framework of a Markovian representation.[12–14] Specific stochastic variables can be employed for describing the instantaneous configuration of the local solvent structure. Solutions in semi-analytic form have been obtained which are suitable for an analysis of optical spectroscopic observables sensitive to the fast librational motions induced by the local cage structure, as observed with far infrared spectra.[13]

Perspectives to novel approaches

There are several possible levels of extension to present theoretical approaches which are worthwhile to be addressed, and which could provide a dramatic improvement in the present interpretative tools available to the physical chemist. Any true advance in the application of theoretical/computational approaches to the interpretation of optical spectroscopies in solution must be based on a combination of the statistical-thermodynamic description of the solvent and advanced determination of molecular structural properties.

First of all, at a basic level of integration (1), it is possible to combine present state-of-the-art quantum mechanical and stochastic approaches in an integrated scheme. A refined computational treatment is then based on a computational approach, which combines *(i)* quantum mechanical calculations of structural parameters (molecular shape, dipole moments, Franck–Condon factors), including environmental and fast vibrational and librational averaging; *(ii)* direct feeding of calculated molecular parameters into stochastic modelling. Integration of all those building blocks defines a reliable computational approach for the *ab initio* prediction of structures, vibrations, and spectroscopic properties of organic molecules in solution. Notice that, in principle, solvent effects can be dealt with in the determination of structural parameters, leaving to the stochastic model the description of slowly relaxing dynamics only; or structural properties can be determined *via* quantum mechanical methods *in vacuo*, allowing for semi-classical corrections in the stochastic model, as we shall show in an example discussed in the following.

Next, at a further level of sophistication (2), we may consider the generalization of current implicit solvent methods—which are essentially static—by including collective solvent dynamics, employing correct non-equilibrium statistical arguments. This is by no means a trivial accomplishment. In practice we seek a 'dynamic equivalent' of the PCM based on a self-consistent definition of a phenomenological theory which includes the full description of an electrohydrodynamic fluid and the time-dependent description of the solute. Finally, a substantially advanced step (3) would be the full development of effective quantum–stochastic approaches, which deal already at quantum mechanical level in a self-consistent way with dissipation and its main effects on spectroscopic observables. This is a fascinating theoretical development, which, however, is at present hardly applicable to real-life experimental problems.

The present paper is essentially devoted to the description of some paradigmatic cases, within the limited scope of level 1, chosen to illustrate the potential, as well as some current limitations, of an integrated approach, which includes as fundamental building blocks *(i)* an accurate determination of structural and electronic properties of different electronic states *via* DFT and TD-DFT methods; *(ii)* evaluation of solvent effects *via* PCM approaches; *(iii)* inclusion of short-time dynamics (vibrations) and *(iv)* description of long-range dynamics *via* stochastic modelling. The focus we have chosen,

namely UV/vis spectroscopy of organic molecular systems, has implications both on the kind of experimental spectroscopic techniques, and on the level of computational description. As case studies, we consider examples of interpretation of the absorption and fluorescence emission spectra of organic molecules in solvated environments to show the necessity of including dynamical processes that occur on a time-scale comparable to that of the spectroscopic transition. In particular we address briefly the interpretation of absorption spectra of topotecan, coumarin, and acrolein, together with dual fluorescence emission of (*N*,*N*′-dimethylamino)benzonitrile (DMABN) in polar solvents. Each case is chosen to clarify the building blocks discussed above, within the established limitations. Finally, we discuss briefly an example of full application of the integrated approach, within the mentioned limitations, namely the fluorescence emission of 4-(1-aza-4,7,10,13-tetraoxacyclododecyl)benzonitrile (DMABN-Crown5).

QM and dynamic modelling of excited states

QM calculations of excited states

The recent implementation of analytical gradients for the time-dependent extension of density functional theory (TD-DFT)[15] allows for the determination of the excited state stationary points and their properties (*e.g.* the multipole moments), with good agreement with experiments. Indeed, while post-Hartree–Fock treatments remain as state-of-the-art approaches to the determination of electronic states of relatively small molecular systems, their computational cost becomes unwieldy when larger molecules are considered. Therefore, TD-DFT is becoming increasingly accepted as a reference computational method. Harmonic frequencies can be obtained from numerical differentiation of analytic gradients, and the subsequent vibrational analysis has provided encouraging results for several systems. On the other hand, there are cases in which DFT exhibits some deficiencies in properly describing excited states involving charge separation, or with substantial contributions from double excitations, not to speak of Rydberg transitions.[16] However, for electronic transitions which involve only partial intramolecular charge-transfer, the underestimation of the excitation energies by TD-DFT, possibly due to spurious self-interaction, may be controlled by the use of hybrid functionals. An example is given by DMABN (see Fig. 1), which is characterized by the presence of two different electronic transitions, depending on the solvent. The first one is a local excitation, whereas the second one is characterized by a non-negligible intramolecular charge-transfer.

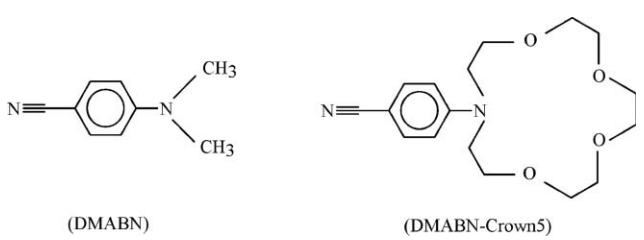

Fig. 1 Molecular structures of (*N*,*N*′-dimethylamino)benzonitrile (DMABN) and 4-(1-aza-4,7,10,13-tetraoxacyclododecyl)benzonitrile (DMABN-Crown5).

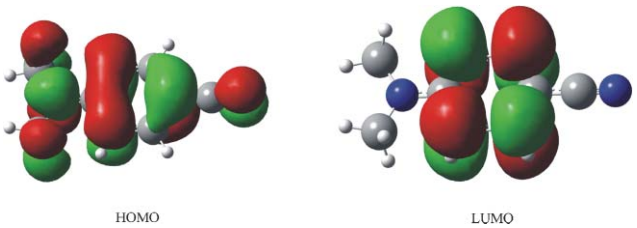

Fig. 2 Frontier orbitals of DMABN.

As shown in Fig. 2, the orbitals involved in the charge-transfer transition (HOMO and LUMO) partially overlap and this could allow a reliable treatment at the TD-DFT level.

Actual calculations performed using the PBE0[17] functional confirm that, provided that diffuse functions are used, the errors w.r.t. experiment are comparable for the charge-transfer and locally excited states, and are close to that delivered by the expensive multireference CASPT2 and CIPSI approaches[18] (see Table 1).

The accuracy of the computational results depends on the density functional employed and PBE0 generally performs very well for valence excitations even involving open-shell species. This latter statement is confirmed from the results collected in Table 2 for the benzoquinone anion radical.

TD-DFT computations predict, in agreement with previous post-HF computations, the presence of two low-lying dark excited states ($1\ ^2B_{2u}$ and $1\ ^2B_{3g}$) around 2.3 eV and two bright states of comparable strength ($1\ ^2B_{3u}$ and $1\ ^2A_u$) around 3 eV. From a quantitative point of view, the average difference between TD-DFT and post-HF results is smaller than that between CASPT2 and SAC-CI values. Comparison between vertical and adiabatic transition energies shows that the effect of geometry relaxation for the excited electronic states is not negligible (around 0.2 eV) and is very similar from TD-DFT

Table 1 Absorption energies (eV) for DMABN *in vacuo* at the TD-DFT level, employing the PBE0 functional and different basis sets, are compared with multireference (CASPT2 and CIPSI) and experimental results

	Local excited	Charge transfer
Experiment	4.35 ± 0.1	4.56 ± 0.1
6-31G(d)	4.68	4.85
6-311+G(d,p)	4.49	4.72
aug-cc-pVTZ	4.45	4.71
CASPT2	4.05	4.41
CIPSI	4.29	4.78
Main contr.	HOMO → LUMO + 1	HOMO → LUMO

Table 2 Vertical excitation energies (in eV) of the benzoquinone anion radical computed in the gas phase by TD-DFT, CASPT2 (from ref. 19) and SAC-CI (from ref. 20) approaches. Adiabatic transition energies are given in parentheses

State	TD/PBE0	CASPT2	SAC-CI
$1\ ^2B_{2u}$ (n/π^*)	2.31	2.23	2.44
$1\ ^2B_{3g}$ (n/π^*)	2.36	2.25	2.38
$1\ ^2B_{3u}$ (π/π^*)	3.09 (2.88)	2.80 (2.61)	2.71
$1\ ^2A_u$ (π/π^*)	3.05 (2.79)	2.82 (2.59)	3.50

and CASSCF computations. Since hybrid density functionals offer also a reliable description of geometric parameters and vibrational frequencies,[10,11] the route seems paved for more ambitious targets, like the simulation of complete spectra involving solvent effects and vibrational contributions (*e.g.* Franck–Condon factors).

Solvation models

As mentioned above, bulk solvent effects can be taken into account by the PCM. A PCM formulation directly applicable to TD-DFT calculations does exist,[3] and it has been successfully applied to the study of the spectroscopic behaviour of several chemical systems in solution.[4] Furthermore, analytical first derivatives have been recently implemented,[15] allowing for effective excited state geometry optimizations.

When dealing with excited states properties in solution, it is important to take solvent relaxation time into proper account.[21] A simple, but very used approach is to define two limit-regimes for the solvent degrees of freedom: the non-equilibrium and the equilibrium regime. The former is more suitable for treating the solvent reaction field to sudden variations of the solute electronic density (as those involved in an electronic transition). The latter corresponds to processes slow enough to allow the whole solvent nuclear relaxation. In this case, all the solvent degrees of freedom are in equilibrium with the electron density of the state of interest.

Both equilibrium and non-equilibrium effects can be treated within the framework of the PCM. The solvent reaction field in the non-equilibrium regime depends on the dielectric constant at optical frequency (ε_{opt}), usually related to the square of the solvent refractive index n ($\varepsilon_{opt} = n^2$). PCM equilibrium solvation is instead ruled by the static dielectric constant (ε). More complex time-dependent solvation effects require proper dynamic models, as described in the next section. Finally, it is worthy of mention that in several systems bulk solvent effects are not sufficient for an accurate treatment of the static and dynamic contributions to excited state properties. In those cases, the inclusion of a limited number of explicit solvent molecules of the cybotactic region is usually sufficient to restore the agreement between computation and experiments.

Let us consider, for purposes of illustration, an example in which even a semi-quantitative approach (*i.e.* vertical excitations with a basic non-equilibrium solvent model) provides results of remarkable interest for the individuation of spectroscopic signatures in large molecules of biological interest. Topotecan is the most commonly used agent for the treatment of ovarian carcinoma, and is the only single agent currently approved in the United States for the treatment of small-cell lung cancer recurrent disease, which is among the most lethal malignancies. Since the drug displays a high degree of toxicity also against normal tissues that show enhanced proliferative rates, a deeper understanding of structure–property relationships is of considerable interest. At concentrations low enough to avoid dimer formation, tautomeric forms with charge +1 (see Fig. 3) dominate in the pH range 4–6.

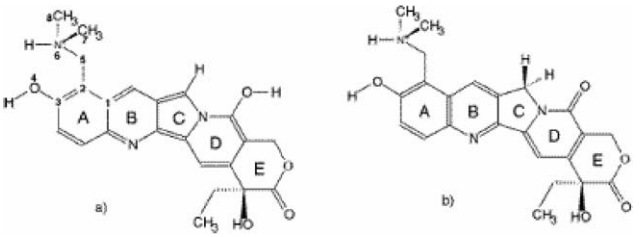

Fig. 3 Molecular structures of topotecan: (a) *eno* form; (b) *keto* form.

QM computations *in vacuo* lead to a single energy minimum corresponding to the *eno* tautomer, whereas inclusion of solvent effects through PCM permits the finding of an energy minimum for the *keto* tautomer that is even more stable than the *eno* one. In Fig. 4 we report the spectra obtained from TD-DFT computations in which each transition is represented by a Gaussian with a half-bandwidth of 10 nm. Panel A clearly shows that the experimental positions of the peaks (dotted lines in Fig. 4) are well reproduced only by the *keto* tautomer, especially in the region 280–600 nm, with the exception of the shoulder at 368 nm (which is related to specific solute–solute–solvent interactions). The essential role played by bulk solvent effects can be appreciated by comparing the computed absorption spectra of the *keto* tautomer either with or without the PCM.

These data (Fig. 4B) show that the spectrum computed *in vacuo* does not reproduce all the experimental results. Besides confirming the reliability of the TD-DFT/PCM

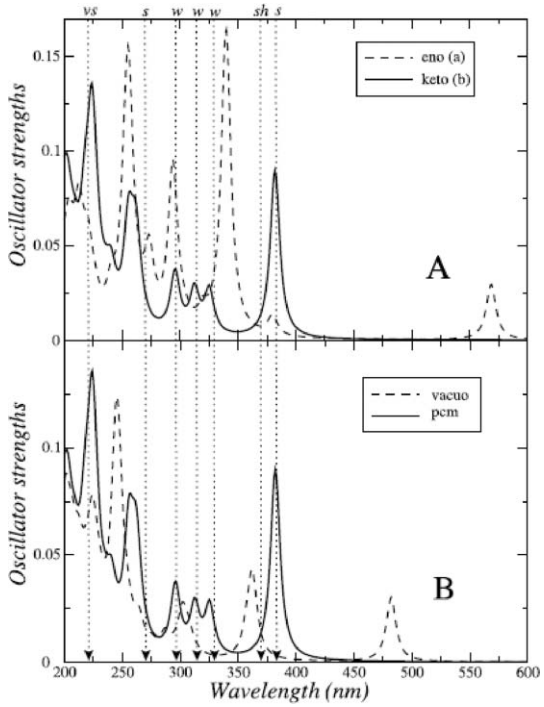

Fig. 4 TD-DFT absorption spectra of: (A) *eno* (dashed line) and *keto* (solid line) forms of topotecan including bulk solvent effect by PCM; (B) *keto* form of topotecan *in vacuo* (dashed line) and in solution (solid line). Dotted lines refer to the absorption band maxima of the experimental spectrum at pH = 5 (legend: (vs) very strong; (s) strong; (w) weak; (sh) shoulder).

approach, the above results have also a significant applicative interest, since the band around 380 nm can be used as a reliable diagnostic of the presence of the *keto* form.

Computation of continuous-wave spectra

Optical continuous-wave (CW) spectra measure the intensities of radiative transitions between molecular stationary states. It is thus possible to compute them relying entirely on a time-independent approach (an alternative route is possible, see next subsection). We focus here on absorption spectra but the computation of fluorescence spectra is completely analogous. The energy-domain expression for the stick absorption spectrum from the electronic state $|e'\rangle$ to $|e\rangle$ is

$$\sigma_{\mathrm{abs}} = \frac{4\pi^2\omega}{3c}\sum_{j',j} p_{j'}\left|\mu_{j',j}\right|^2 \delta\left(E_{j'} - E_j + \hbar\omega\right) \qquad (1)$$

where $\mu_{j',j} = \langle j'|\langle e'|\mu|e\rangle|j\rangle$ are the transition dipole moments, $|j'\rangle$ and $|j\rangle$ are the vibrational states of $|e'\rangle$ to $|e\rangle$ respectively, $E_{j'}$ and E_j their energies and $p_{j'}$ the Boltzmann population of initial states $|j'\rangle$. In condensed phase, finite-time relaxation of the solvent can indeed affect the spectrum by modulating the energies and wave-functions of the vibrational states $|j\rangle$. Therefore, it is useful to adopt the approach of the two time-regime limits described in the previous section, and to define consequently non-equilibrium $\sigma_{\mathrm{abs}}^{\mathrm{neq}}$ and equilibrium $\sigma_{\mathrm{abs}}^{\mathrm{eq}}$ limits to the spectrum.[21] In line of principle the non-equilibrium limit is more suited for absorption spectra. Nonetheless, when dealing with fluorescence spectra, the ability to describe equilibrium/non-equilibrium regimes and possible intermediate cases, can make calculation of spectra a powerful, though indirect, tool to investigate solvation dynamics for large systems. As mentioned above, state-of-the-art TD-DFT calculations allow a complete and balanced description of the molecular vibrations of ground and excited electronic states for medium/large-size molecules, also in the condensed phase when coupled to PCM.[22] Transition moments can therefore be computed if one is able to evaluate Franck–Condon overlaps among generic vibrational states of the involved electronic states. While the basic algorithm performing such a task is well known, its extension to large systems is by no means trivial due to the exponential increase in the number of vibrational states to be taken into account. However, an effective solution to this problem has been recently proposed, based on reliable *a priori* estimates of the integrals to be computed.[23]

As an example, we consider the widely investigated case of coumarin 153 (C153) in two solvents of different polarities (cyclohexane and dimethyl sulfoxide, DMSO). The spectra are dominated by a strongly allowed transition for which the Condon approximation (transition dipole independent on the nuclear coordinates) can be considered fully adequate. The 0–0 transition energies computed in the gas phase by the PBE0 functional for the nearly isoenergetic *syn* and *anti* isomers are 25 680 and 25 660 cm^{-1}, in almost quantitative agreement with the experimental values (25 898 and 25 710 cm^{-1}, respectively).[24] Furthermore, the calculated values for the oscillator strength (0.36 and 0.37, respectively) match their experimental counterpart (0.37) very well.[25] PCM/TD-PBE0 calculations predict that both in DMSO and in cyclohexane the dipole moment shift associated to the electronic transition is about 6 Debyes. This value is in good agreement with the estimates based on electroabsorption experiments[26] and slightly underestimated with the experimental determination in the gas phase,[27] supporting the reliability of the suggested computational approach.

The absorption spectra computed in DMSO and cyclohexane are compared in Fig. 5 to their experimental counterparts. The presence in the cyclohexane spectrum of two strong features with comparable intensity spaced by about 1300 cm^{-1} is well reproduced and this is also the case for the coalescence into a single peak accompanied by a significant blue-shift issuing from passage from cyclohexane to DMSO solvent. From a quantitative point of view, the computed band maxima are blue-shifted by about 400 cm^{-1} from experimental values, whereas the only qualitative discrepancy concerns the relative heights of the two peaks observed in cyclohexane. As a matter of fact, the first peak is mainly due to the contribution from the 0–0 transition together with an overtone involving a cooperative ring vibrational mode n18 with a frequency (383 cm^{-1}) very close to that of a strong feature found in the gas-phase dispersed fluorescence spectrum (380 cm^{-1}).

Stochastic models

Understanding of relaxation processes of solutes in liquids can be addressed in terms of many-body Fokker–Planck models, which describe, in the framework of Markovian representation, the joint dynamics of a single molecule, *probe*, with solvation coordinates which can represent, for instance, a local cage structure formed by the solvent surrounding the probe, polarization coordinates describing the fluctuating field around the probe in polar media, or local domains in protein environments. Standard Brownian motion theory, with the solvent appearing as a mere source of frictional drag, is not sufficient as long as it neglects the persistent (on the short time-scale of the librational motions) torques due to the solvation cage structure. In recent works the method of the stochastic cage model has been developed with the purpose of describing the effects of the local solvent structure in the framework of a Markovian representation. Specific stochastic variables are employed for describing the instantaneous configuration of the

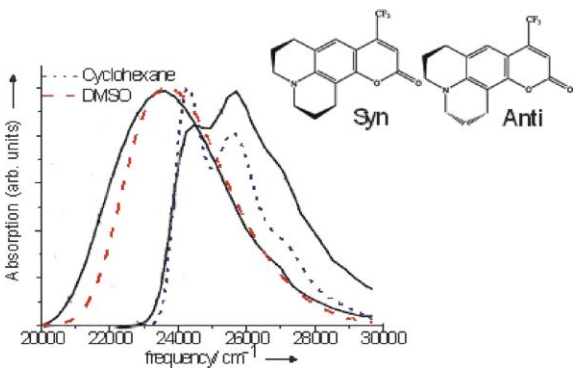

Fig. 5 Comparison between experimental (black lines) and computed (dotted and dashed lines) spectra of C153 in different solvents. Computed spectra are red-shifted by 400 cm^{-1}.

local solvent structure: the cage orientation (*i.e.* the equilibrium orientation within the cage of the solute or of the probe) and the librational frequency as a measure of the strength of solute–solvent interactions. This method can be applied to both translational and rotational motions at different levels of approximation depending, on the one hand, on the detail in the description of the cage dynamics and, on the other hand, on the accuracy in the calculation of the relevant observables. A generic time evolution equation for the conditional probability $P(Q_0,0|Q,t) \equiv P(Q,t)$ of a molecular system described by stochastic coordinates Q is in general written as:

$$\frac{\partial}{\partial t}P(Q,t) = -\hat{\Gamma}P(Q,t) \qquad (2)$$

Here $\hat{\Gamma}$ is the time evolution operator dictating the dependence upon the set of coordinates Q of the probability of the system at time t, which admits a time-independent (equilibrium) solution with a generic Boltzmann form $P_{eq}(Q)$ defined with respect to the total energy $E(Q)$.

Application of stochastic models to the evaluation of dynamic and stationary emission fluorescence spectra of solvated molecules can be formalized as follows. The emission spectra $I(t)$ is in general written as an integral over ground and excited state phase space variables. For a given configuration of the excited state, e, a generic signal for fluorescence emission to ground state, g, promoted by absorption with depolarized light is given by

$$I \propto \omega^3 \int \mathrm{d}Q k^{\mathrm{rad}}_{\mathrm{e}\to\mathrm{g}}(Q) g[\omega - \Delta\omega(Q)] P(Q,t) \qquad (3)$$

multiplied by a constant factor depending upon the experimental apparatus. In eqn (3) $g[\omega - \Delta\omega(Q)]$ is a function describing the shape of the band centered on frequency $\Delta\omega(Q)$ given in terms of state energies, *e.g.* $\Delta\omega(Q) = E_e(Q) - E_g(Q)$. The excited state population $P(Q,t)$ is described by a time evolution equation which is based on the stochastic operator $\hat{\Gamma}$, plus the relaxation processes affecting the excited state: a source term $S(Q,t)$ for the creation of excited state population and an emission term $k(Q) = k^{\mathrm{rad}}_{\mathrm{e}\to\mathrm{g}}(Q) + k^{\mathrm{nr}}_{\mathrm{e}\to\mathrm{g}}(Q)$ to account for radiative and non-radiative decay.

As an example of this approach, let us consider the fluorescence of DMABN. Since the initial discovery by Lippert *et al.*[28] of the dual fluorescent behavior of DMABN in polar solvents, the molecule has been the subject of numerous experimental and theoretical studies aimed to explain the anomalous fluorescence.[29–33] The emission spectra of DMABN present two fluorescence bands strongly dependent on the polarity of solvent and temperature. In solvents with low polarity, only a band called LE (locally excited) is observed at short-wavelength while in high polarity solvents a band called TICT (twisted intramolecular charge transfer) is found at long-wavelength, whereas the band at short-wavelength disappears. The long-wavelength fluorescence, as with all typical TICT emissions, undergoes a strong red-shift with the increase in the polarity of the solvent. These evidences can be explained with Grabowski's model[32] or TICT model: the excited state presents two different metastable states (planar, related to LE emission, and perpendicular, related to TICT emission) that can interconvert by a torsional motion. A continuous stochastic model can be used to describe the charge-transfer dynamics of the excited state which accompanies torsional motion.[34,35]

The stochastic model reproduces the static spectra of DMABN in solvents with different polarities, and their temperature dependence. As an example, the calculated temperature dependence of DMABN emission spectra in *n*-butyl chloride is shown in Fig. 6. The emission profile exhibits a minimum around 180–200 K for the LE band and this is a direct consequence of competition between the decay to the ground state and the interconversion to the TICT state.

Toward an integrated QM/stochastic approach

In order to illustrate the initial results of an integrated QM/stochastic approach, let us consider the fluorescence spectrum of DMABN-Crown5 (*cf.* Fig. 1), which shows two bands in medium polarity solvents which can be interpreted as TICT and LE signals.

Basic ingredients for the definition of the computational model and the direct evaluation of fluorescence emission spectra are (1) the potential energy surfaces (PES) obtained from QM calculations in the ground and excited states in the gas phase and for different solvents; (2) diffusion tensor D_φ for the internal conformational diffusive motion, which can be evaluated using hydrodynamic arguments; and finally (3) solvent polarization diffusion which is described by diffusion tensor D_S, which can be related to solvent relaxation times.

In the previous sections, we have seen that the TD-DFT/PCM approach is able to provide reliable PES for the relevant electronic states. Thus, selection of a relevant set of stochastic coordinates is the most crucial step in the definition of the model and the corresponding time evolution operator. In the case of rigid fluorescent systems, a Brownian diffusion model includes explicitly the orientation of the solute $\boldsymbol{\Omega}$. Additional internal degrees of freedom φ can be added to describe the dynamic evolution of dihedral angles and/or more complex conformational motions. Dynamic solvent coordinates can be represented simply by a local solvent polarization vector.

In Fig. 7, a cartoon of the relevant degrees of freedom employed for interpreting dual fluorescence of DMABN-Crown5 derivatives is shown. In general, the molecular orientation $\boldsymbol{\Omega}$ is coupled to the dynamic solvent vector variable

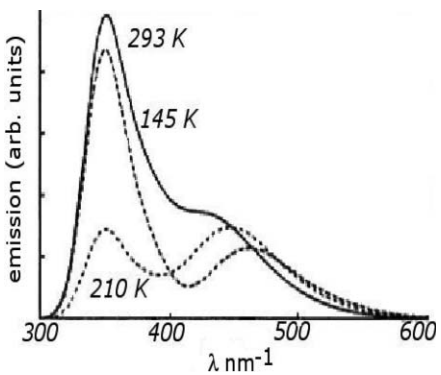

Fig. 6 Calculated temperature dependence of DMABN emission spectra in *n*-butyl chloride.

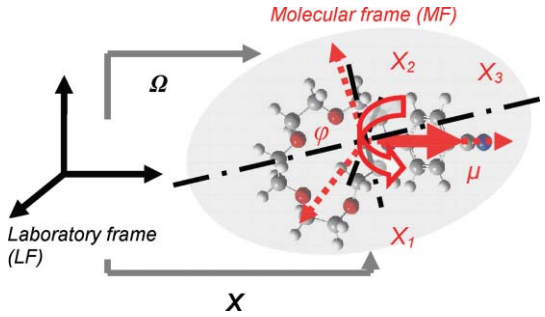

Fig. 7 Relevant degrees of freedom for modelling 4-(1-aza-4,7,10,13-tetraoxacyclododecyl)benzonitrile (DMABN-Crown5) fluorescence. Orientation is given by a set of Euler angles $\boldsymbol{\Omega}$; relative orientation of donor–acceptor groups are described by the torsional angle φ; a stochastic vector coordinate $\boldsymbol{X}$ represents the solvent relaxation.

$\boldsymbol{X}$ and the internal conformational angle φ. In polar isotropic fluid, coupling with rotational coordinates can be averaged out, while only one component of the solvent polarization variable is tightly coupled to the molecular electric dipole. The time evolution operator describing the molecule dynamics is defined as a diffusive operator which includes the internal rotation and the solvent relaxation, following standard procedures.[13,14]

The structures of the five most stable conformers of DMABN-Crown5 have been optimized in the gas-phase at the PBE0/6-31G(d) level (Fig. 8). Vertical excitation energies to the first and second excited states have been calculated by the same functional and basis set using the TD-DFT approach. The investigation of the PES for the ground and the excited states, mainly regarding dependence from the torsional angle, has been performed on the optimized gas-phase structures of the ground electronic state. At each geometry the dipole moments for ground and excited states are computed, as well.

Emission fluorescence is calculated by solving a diffusion/sink/source equation analogous to eqn (2) for the stationary populations of the excited states.

Spectra have been calculated in five different solvents of different polarities: DMSO, acetonitrile, dichloromethane, cyclohexane and *n*-octanol. A preliminary comparison of

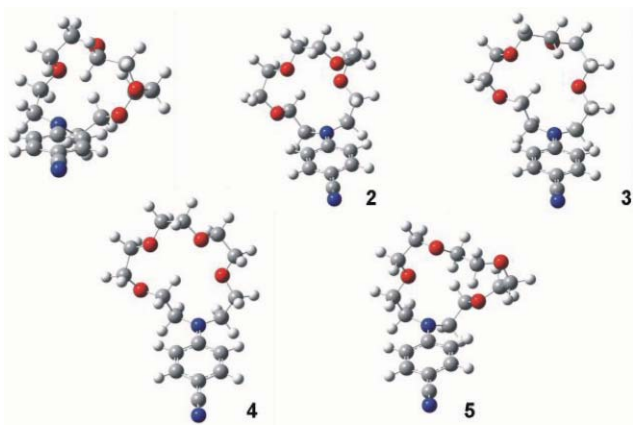

Fig. 8 Representative low-energy conformations of 4-(1-aza-4,7,10,13-tetraoxacyclododecyl)benzonitrile (DMABN-Crown5).

Table 3 Experimental[36] and calculated positions of emission maxima for DMABN-Crown5 in different solvents

	Exp. maximum/s^{-1}	Calc. maximum/s^{-1}
DMSO	6.33×10^{14}	6.40×10^{14}
Acetonitrile	6.47×10^{14}	6.42×10^{14}
n-Octanol	6.70×10^{14}	6.64×10^{14}
Dichloromethane	6.79×10^{14}	6.75×10^{14}
Cyclohexane	8.61×10^{14}	8.63×10^{14}

experimental[36] and calculated[37] spectra is encouraging, allowing evaluation of relevant emission peaks.

A quantitative comparison of the fluorescence spectra is given in Table 3, which reports the predicted locations of emission maxima in the considered solvents.

The spectrum in cyclohexane is characterized by a fluorescence maximum at 8.61×10^{14} s^{-1}. Spectra in all other solvents show two bands: one around 8.64×10^{14} s^{-1} and another between 6.79×10^{14} s^{-1} and 6.33×10^{14} s^{-1}. The latter peak shifts towards lower frequency as the dielectric constant of the solvent increases, while at the same time the ratio of the two peak intensities increases. All these features are reproduced reasonably well by the computational model.

Conclusions

The relationship between spectroscopic measurements and molecular properties can be gathered only indirectly, that is, structural and dynamic molecular characteristics can be inferred from the systematic application of modelling and numerical simulations to interpret experimental observables. A straightforward way to achieve this goal is the employment of spectroscopic evidence as the 'target' of a fitting procedure of molecular, mesoscopic and macroscopic parameters entering the model. This strategy, based on the idea of a general fitting approach, can be very helpful in providing detailed characterization of molecular parameters.

A more refined methodology is based on an integrated computational approach, *i.e.* the combination of quantum mechanical calculations of structural parameters, possibly including environmental and fast vibrational and librational averaging, and direct feeding of calculated molecular parameters into dynamic models based on molecular dynamics, coarse grain dynamics, and stochastic modelling or a combination of the three.

Our main objective in this review has been to discuss the degree of advancement in the integrated computational approach to the interpretation of absorption and fluorescence emission of organic molecules in solvated environments, *via* combination of advanced quantum mechanical approaches and stochastic modelling of relaxation processes.

From the quantum mechanical point of view, methods rooted in the density functional theory are able to reproduce with good accuracy structures and most optic spectroscopic parameters of large molecules, provided that static bulk solvent effects are taken into account by continuum models like the polarizable continuum model. Inclusion of some explicit solvent molecules (together with the continuum) allows one to take into the proper account specific solute–solvent interactions. Long-range relaxation processes, which are of

fundamental importance to interpret correctly emission fluorescence of flexible molecules, have been related to stochastic modelling. Specific stochastic variables are employed for describing the instantaneous configuration of the local solvent structure and numerical solutions in semi-analytic form can be obtained in terms of correlation functions which are directly linked to spectroscopic observables.

Integration of all these building blocks can be used to define a robust and reliable computational approach for *ab initio* prediction of both absorption and emission spectroscopic properties of organic molecules in solution.

References

1 W. Koch and M. C. Holthausen, *A chemist's guide to density functional theory*, Wiley-VCH, Weinheim, 2nd edn, 2001.
2 R. Improta and V. Barone, *Chem. Rev.*, 2004, **104**, 1231.
3 J. Tomasi, B. Mennucci and R. Cammi, *Chem. Rev.*, 2005, **105**, 2999.
4 N. Sanna, G. Chillemi, A. Grandi, S. Castelli, A. Desideri and V. Barone, *J. Am. Chem. Soc.*, 2005, **127**, 15429.
5 O. Crescenzi, M. Pavone, F. de Angelis and V. Barone, *J. Phys. Chem. B*, 2005, **109**, 445.
6 G. Brancato, N. Rega and V. Barone, *J. Chem. Phys.*, 2006, **125**, 164515.
7 R. Car and M. Parrinello, *Phys. Rev. Lett.*, 1985, **55**, 2471.
8 N. Rega, S. S. Iyengar, G. A. Voth, H. B. Schlegel, T. Vreven and M. J. Frisch, *J. Phys. Chem. B*, 2004, **108**, 4210.
9 N. Rega, G. Brancato and V. Barone, *Chem. Phys. Lett.*, 2006, **422**, 367.
10 V. Barone, *J. Chem. Phys.*, 2005, **122**, 014108.
11 V. Barone, P. Carbonniere and C. Pouchan, *J. Chem. Phys.*, 2005, **122**, 224308.
12 L. D. Favro, *Phys. Rev.*, 1960, **119**, 53; P. S. Hubbard, *Phys. Rev. A: At. Mol. Opt. Phys.*, 1972, **6**, 2421; M. Fixman and K. Rider, *J. Chem. Phys.*, 1969, **51**, 2429.
13 A. Polimeno and G. J. Moro, *J. Chem. Phys.*, 1994, **101**, 703.
14 G. J. Moro and A. Polimeno, *J. Chem. Phys.*, 1997, **107**, 7884.
15 C. Van Caille and R. D. Amos, *Chem. Phys. Lett.*, 1999, **308**, 249; C. Van Caille and R. D. Amos, *Chem. Phys. Lett.*, 2000, **317**, 159; T. Tsuneda and K. Hirao, *J. Chem. Phys.*, 2006, **124**, 144106.
16 A. Drew and M. Head-Gordon, *Chem. Rev.*, 2005, **105**, 4009.
17 C. Adamo and V. Barone, *J. Chem. Phys.*, 1999, **110**, 6158.
18 L. Serrano-Andrés, M. Merchán, B. O. Roos and R. Lindh, *J. Am. Chem. Soc.*, 1995, **117**, 3189; B. Mennucci, A. Toniolo and J. Tomasi, *J. Am. Chem. Soc.*, 2000, **122**, 10621.
19 R. Pou-Amérigo, L. Serrano-Andrés, M. Merchán, E. Ortí and N. Forsberg, *J. Am. Chem. Soc.*, 2000, **122**, 6067.
20 Y. Honda, M. Hada, M. Ehara and H. Nakatsuji, *J. Phys. Chem. A*, 2002, **106**, 3838.
21 T. Fonseca, H. J. Kim and J. T. Hynes, *J. Photochem. Photobiol., A*, 1994, **82**, 67; M. Cossi and V. Barone, *J. Chem. Phys.*, 2001, **115**, 4708.
22 G. Scalmani, M. J. Frisch, B. Mennucci, J. Tomasi, R. Cammi and V. Barone, *J. Chem. Phys.*, 2006, **124**, 094107.
23 R. Improta, V. Barone and F. Santoro, *Angew. Chem., Int. Ed.*, 2007, **46**, 405; F. Santoro, A. Lami, R. Improta, J. Bloino and V. Barone, *J. Chem. Phys.*, 2007, **126**, 084509.
24 B. A. Pryor, P. M. Palmer, Y. Chen and M. R. Topp, *Chem. Phys. Lett.*, 1999, **299**, 536.
25 A. Muhlpfordt, R. Schanz, N. P. Ernsting, V. Farzdtinov and S. Grimme, *Phys. Chem. Chem. Phys.*, 1999, **1**, 3209.
26 A. Chowdury, S. A. Locknar, L. L. Premvardham and L. A. Peteanu, *J. Phys. Chem. A*, 1999, **103**, 9614.
27 K. Kanya and Y. Ohshima, *Chem. Phys. Lett.*, 2003, **370**, 211.
28 E. Lippert, W. Lüder, F. Moll, W. Nagele, H. Boos, H. Prigge and I. Seibold-Blankenstein, *Angew. Chem.*, 1961, **73**, 695.
29 M. Van Der Auweraer, Z. R. Grabowski and W. Rettig, *J. Phys. Chem.*, 1991, **95**, 2083.
30 M. Van Der Auweraer, A. Vannerem and F. C. De Schryver, *J. Mol. Struct.*, 1982, **84**, 343.
31 Z. R. Grabowski, K. Rotkiewicz, A. Siemiarczuk, D. J. Cowley and W. Baumann, *Nouv. J. Chim.*, 1979, **3**, 443; Z. R. Grabowski, *Pure Appl. Chem.*, 1992, **64**, 1249.
32 Z. R. Grabowski, K. Rotkiewicz and W. Rettig, *Chem. Rev.*, 2003, **103**, 3899.
33 A. L. Sobolewski, W. Sudholt and W. Domcke, *J. Phys. Chem. A*, 1998, **102**, 2716.
34 A. Polimeno, A. Barbon, P. L. Nordio and W. Rettig, *J. Phys. Chem.*, 1994, **98**, 12156.
35 A. Polimeno, G. Saielli and P. L. Nordio, *Chem. Phys.*, 1998, **235**, 313.
36 E. Lippert, W. Rettig, V. Bonačić-Koutecký, F. Heisel and J. A. Miehé, *Adv. Chem. Phys.*, 1987, **68**, 1.
37 S. Carlotto, C. Ferrante, M. Maggini, A. Polimeno, C. Benzi and V. Barone, in preparation.